IEEE Access
Multidisciplinary | Rapid Review | Open Access Journal

Received November 28, 2018, accepted December 29, 2018, date of publication January 18, 2019, date of current version February 6, 2019.

Digital Object Identifier 10.1109/ACCESS.2019.2892816

Molecular-Based Nano-Communication Network: A Ring Topology Nano-Bots for In-Vivo Drug Delivery Systems

DANIEL TUNÇ MCGUINESS, VALERIO SELIS, (Member, IEEE), AND ALAN MARSHALL, (Senior Member, IEEE)

Department of Electrical Engineering and Electronics, University of Liverpool, Liverpool L69 3GJ, U.K.

Corresponding author: Daniel Tunç McGuiness (d.t.mcguiness@liverpool.ac.uk)

This work was supported by the Engineering and Physical Sciences Research Council through Creating a Stink-Investigating Olfactory Transport Streams under Grant EP/M029425/1.

ABSTRACT Compared to traditional machines in computer networks, nano-bots in nano-networks face challenges due to the limitations of processing capabilities and power management. Under these limitations, these nano-bots can only perform simple tasks. Use of nano-bots can be applied to fields such as environmental, biomedical, and industrial fields. However, to use nano-bots in practice, their management and control in nano-networks should be established. In this paper, a network protocol for use in *in-vivo* communications applied to drug-delivery systems is proposed. Based on the circulatory system, three types of nano-bots are designed to be used in a ring topology network. The physical channel of the communication is discussed in detail, a docking process between nano-bots is proposed, a method to access the channel is presented and simulation results of the communication network are presented.

INDEX TERMS Nano-network, nano-scale communications, nano-bots, in-vivo communications, physical layer, medium access control layer.

I. INTRODUCTION

Drug delivery systems (DDSs) can be defined as a collection of techniques designed for delivering drugs to the desired location in a controlled and quantitative way without disrupting the general function of the host. Recent advances in the fields of nanotechnology [1], biotechnology [2] and biomedical sciences [3] have made great strides in understanding the process and the physical application of this type of delivery system. One promising implementation of drug delivery systems is the use of nano-communication networks.

In literature, nano-communications is achieved in two major propagation paradigms:

- Electromagnetic (EM) propagation
- Molecular (MC) propagation

In the electromagnetic approach, Terahertz (THz) frequencies, has been suggested for nano-bot to nano-bot communication [4]–[9]. However, the effects of electromagnetic radiation on living tissue can be considered a problem in implementing EM based nano-networks for use, even under the current safety limit of 1 mW/cm^2 [10], [11]. The effects on THz radiation in the human body is still an open question, however there are experimental analysis on other species that show DNA damage and induced anxiety under the influence of short term THz radiation [12]–[14]. A final note to address is the source of radiation relative to the living organism. The human body has adaptations against electromagnetic radiation if the radiation source is outside the body [15], [16]. However, if the radiation source is originating from inside the human body, its effects are likely worse.

The second approach, Molecular propagation (MC), is the act of using particles as a means of transmission information [17]. This process can be a more suitable option for nano-networks over THz communication which are the energy indepedency of the propagation (i.e. diffusion) and bio-compability. The use of molecular based propagation for nano-network is seldom studied compared to THz where the focus is mostly on the physical layer [18]–[25].

One of the driving forces behind the study of nano-communication networks is its promise of delivering drugs to its precise location quantitatively. Medical applications of MC are reviewed in general in [27]. There can be numerous application of utilizing nano-scale (nm) robots. The potential fields of application can be given as [28];

- **Neurological diseases:** Neurological diseases are usually treated by delivering the drug in the nervous

system. This is not a trivial task as the Blood-Brain-Barrier (BBB) protects the brain against foreign materials [29]–[31]. This makes it difficult to treat different diseases such as traumatic brain injury, multiple sclerosis and epilepsy. One of the most promising strategies utilize nanoparticles that imitates proteins that normally pass the BBB [32]–[34].

- **Genetic diseases:** The use of a drug delivery system for treating genetic diseases via gene therapy can be used in the penetration of the desired genetic information in the patient [35].
- **Human Immunodeficiency Virus:** An important challenge in HIV drug delivery is the degradation and poor penetration in the gastrointestinal (GI) tract [36], [37].
- **Gastro-Intestinal diseases:** Most of the diseases of the GI tract, e.g. ulcerative colitis and Crohn's disease, require advanced drug delivery systems to improve drug delivery processes [38], [39].

There have been various studies conducted in nano-scale communications [40]. These include: synchronization attempts [41], relaying [42], routing [43], [44], Medium Access Control (MAC) [45]–[48] and physical channel properties [49], [50]. It must be noted that, most studies regarding nano-networks assume the propagation is achieved via electromagnetic waves (i.e. THz), even though there are alternatives which may prove to be biologically safer and more secure against outer threats.

As with any electromagnetic communication, there can be outside influences that may hinder the network, cause it to malfunction or force it to behave in ways it was not meant to behave [51]. The use of an EM-only communication between nano-networks also opens up possibilities in which an attacker can take control of the system and therefore the security of nano-networks is still an important and open question [52].

In this study, a novel in-body communication network based on nano-technologies is proposed. There are two main aspects which the proposed network address. Firstly, the network is used to distribute a drug in the body by using static nano-bots which contain a low amount of drug. This removes an issue in the case a nano-bot fails, also, the amount of drug released would not be dangerous for the individual. Secondly, this new communication method removes the necessity of using a large amount of nano-bots communicating via wireless communications based on terahertz, which can negatively affect the human body. In addition, the physical layer in which the nano-bots travel is described and the physical connection process of information exchanged between the travelling nano-bots and stationary nano-bot is described by proposing a novel docking/departing process based on magnetic-locking.

The structure of the paper is as follows. In Section I, an introduction to the study is given. Section II focuses on the nano-bots conceptualized in this study; nano-bot bit, nano-bot node and nano-bot gateway. Section III delves into the architecture of the proposed nano-bots to be used in in-vivo communication. Section IV focuses on the physical layer of the nano-network including the parabolic velocity profile of the flow, the advective propagation and the duration of magnetic docking/departing process, which takes place to realize nano-bot to nano-bot communication possible. The packet protocol is established in Section V and a short section is given for the simulation results on the proposed topology in Section VI and conclusion and future-work is give in section VII.

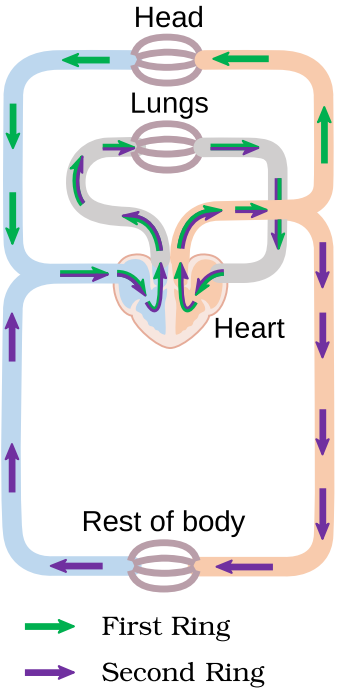

FIGURE 1. A simplified diagram of the circulatory system used in modelling the proposed ring nano-network [26].

II. NANO-NETWORK

The circulatory system can be ideally represented as two ring networks connected together as shown in Figure 1 with a unidirectional flow. A ring network is a particular topology consisting of each node connected to only two nodes in order to create a unique ring path for the packet to flow through.

In the nano-network three types of nano-bots are envisioned:

- *Nano-bot bit (N_b)*: this is the simplest nano-bot which main aim is to carry a drug and/or a particle (bit) in the nano-network. It is a mobile nano-bot which circulates in the system by using the blood vessels. It should be noted that the presence of a particle (bit) represents 1, while its absence represents 0.
- *Nano-bot node (N_N)*: this nano-bot is relatively more complex than the N_b and its main function is to transmit and receive information in the nano-network. It is a static nano-bot which retrieves/injects (read/write) a drug or a particle (bit) from/to a N_b.

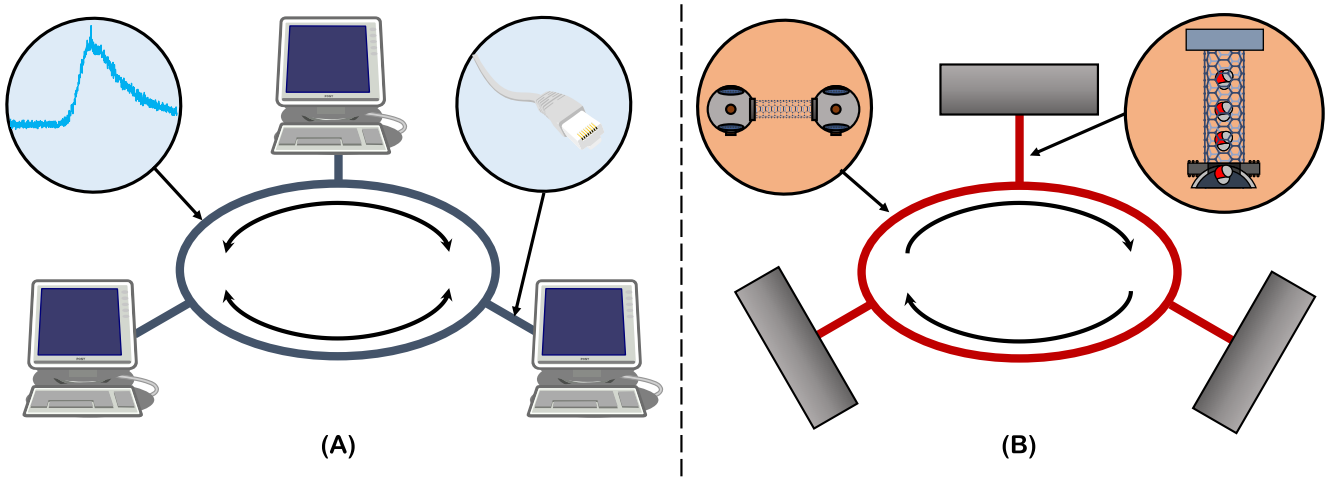

FIGURE 2. Representation of a ring topology for computer network and nano-network (a) A classical ring network in computer communications where each computer shares a common channel to transmit information between each other and the transmission can be done both ways in the channel (i.e. full-duplex) (b) The proposed network topology that can be used in in-vivo communication. Unlike a computer communication, the transmission is unidirectional which forces packets to be transmitted in one rotation.

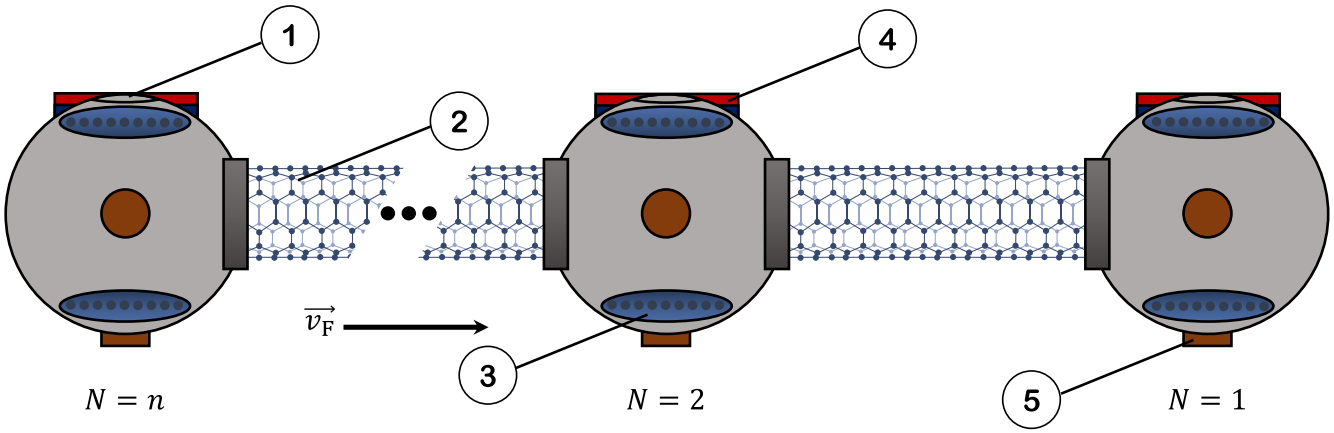

FIGURE 3. Representation of a packet composed by *n* nano-bot bits chained together with nano-tubes. (1) The hatchet where the transmission between the travelling nano-bot and the stationary nano-bot is made (2) The carbon nano-tube that creates stability and elasticity to allow a chain of nano-bots to traverse the circulatory system (3) The piezoelectric nano-generator that allows to generate energy from collisions as it travels (4) is the nano-docking system realized by the magnetic docking/departing process [53]–[55] (5) is the nano-motor that allows for stability and aligning with the stationary bot in docking process [56], [57] [58]–[60].

- *Nano-bot gateway (N_{GW})*: this is the most important nano-bot in the nano-network and has several roles: (i) retrieve the status of the N_N and N_b; (ii) keep count of N_b in the circulatory system; (iii) send this information to external devices in the proximity, e.g. alerting when the amount of drug in the nano-network is insufficient, alerting if an N_N and/or an N_b fails etc. As with the N_N, it is static and located where the two rings intersect, and it retrieves/injects a particle (bit) from/to a N_b for internal communications.

In a computer network the ring topology can be affected by the failure of a node or cable, which will cause the ring to be broken. However, in the nano-network based on the circulatory system, the failure of a node does not affect the entire network as the medium is the blood vessel. In case of a failure or misbehaviour of N_b and/or N_N, it is the N_{GW}'s task to report this to the external world and in some cases to act internally. A graphical representation between a computer network and a nano-network based on a ring topology is shown in Figure 2.

As the circulatory system can be seen as two rings connected together, some of the N_bs will always circulate in the upper ring (first ring in Figure 1) and some will always circulate in the lower ring (second ring in Figure 1).

The generic protocol stack used in the nano-network is composed of three main layers:

- Physical Layer: this is based on molecular-based nano-communications and makes the transmission of bits possible.
- Medium access control (MAC) layer: this provides access to the physical layer and describes how data frames are exchanged in the nano-network.
- Application layer: this provides an interface between the applications running in the static nano-bots and the MAC layer, and it is used for exchanging messages.

The application layer will not be discussed in detail further as it is not the aim of this work.

III. NANO-BOT PHYSICAL ARCHITECTURE

Figures 4 and 5 show the different physical architectures of nano-bots present in the nano-network. The physical architecture of a N_b (Figure 4) consists of several components such as

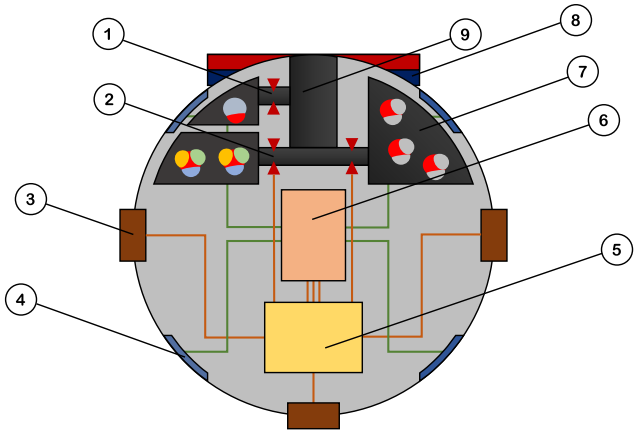

FIGURE 4. Representation of a nano-bot bit: (1) The valve that controls particle-bit box for storing the bit exchanged by nano-bot nodes and the nano-bot gateway; (2) The particle-gw valve that controls the storage for storing the bits for providing the status of the nano-bot bit to the nano-bot gateway; (3) is the nano-motor that allows for stability and aligning with the stationary bot in docking process [56], [57] (4) is the piezoelectric nano-generator that allows to generate energy from collisions as it travels [58]–[60] (5) is the nano-controller unit responsible for the minimum intelligence required for the travelling nanobot to be aware of its surroundings [61]–[63] (6) is the nano-battery that stores excess energy from the piezoelectric nano-generator [64] (7) The drug reservoir (8) is the nano-docking system realized by the magnetic docking/departing process [53]–[55] (9) The main inlet in which particles are sent and received in the information transmission process.

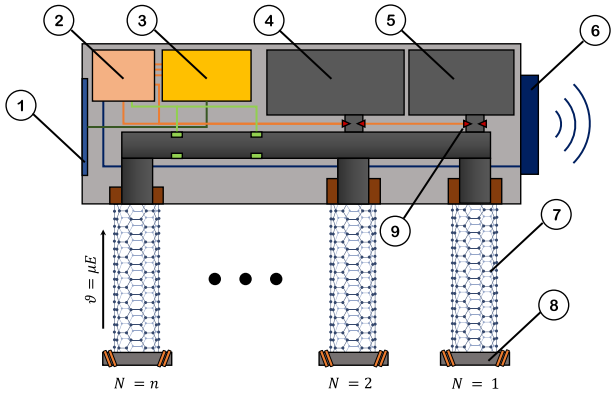

FIGURE 5. Representation of a nano-bot gateway. (1) The nano-bot charges itself from particle collision via piezoelectric nano-generators [58]–[60] (2) The nano-controller responsible for the management of the valves and the "intelligence" aspect of the bot in addition to the sensors present in the nano-bot [61]–[63] (3) The battery unit responsbile of storing excess energy generated from the piezoelectric nano-generators [64] (4) Storage for the information particles (5) Storage for the drug particle. (6) Transmitter to convey information regarding the body to the outside environment (Gateway only) (7) Carbon nano-tube to transmit information between travelling nano-bot and the stationary nano-bot [65] (8) Controllable magnet (i.e. electromagnet) to realize the docking/departing process [53]–[55] (9) Valves controlled by the nano-controller to release drug and/or information particles to the travelling nano-bot.

particle boxes, a drug reservoir, nano-sensors, nano-motors, a nano-docking system, a nano-recharging system and a nano-controller unit.

As the N_b is used to carry a bit, a particular container is required for storing a particle which will be injected/retrieved by a N_N or N_{GW}, called the particle-bit box. A N_b is also used for delivering small quantities of drug when required, for this reason a drug reservoir is necessary for storing it. It is envisioned that a N_b will circulate in the main circulatory system, therefore, the flow in the blood vessel can cause turbulences which can wrongly direct the N_b into capillaries. For this reason, the N_b is equipped with nano-sensors [63] for measuring the velocity of the flow and nano-motors [56], [57] to adjust its direction and maintain the center path of the blood vessel. The motors also allow the bots to remain in the main arteries and avoiding travelling to veins. The nano-docking system is used to attach/detach the N_b to the N_N or N_{GW} in order to exchange particles and drugs. It uses a magnet for stabilising the N_b during the reading/writing process. This is called docking/departing process, which allows connection without any need for detecting the static node. This will be studied in details in Section IV-D. In order to be functional the N_b requires a small amount of energy which is provided by the nano-recharging system. This is composed by four piezoelectric nano-generators [58]–[60] providing clean and renewable energy, which will be stored in a nano-battery [64]. The most important component in the N_b is the nano-controller unit (NCU) [61], [62] which manages the internal components of the N_b. This needs to make sure that the N_b is following the center path of the blood vessel by reading information from the nano-sensors and adjusting the direction by using the nano-motors. The NCU has the responsibility of opening/closing the valves for releasing the correct amount of drug or particles. Another important function is to provide its functional status to the N_{GW}, e.g. battery level, failures etc., by releasing specific particles stored in the particle-gw box. Each N_b will be connected with a nano-tube to another N_b thus forming a chain of N_bs. A representation of this chain is shown in Figure 3 and represents a packet.

Except for the antenna component, Figure 5 shows the physical architecture of a N_N/N_{GW} in which the computational functionalities of a N_b are enhanced. The main difference consists of using an advanced docking system composed by n nano-tubes [66] for retrieving/injecting bits from/to n N_bs. It also consists of electromagnets in order to change the polarity for attaching and detaching N_bs. The particle-bit box and the drug reservoir are bigger than the boxes in a N_b giving the opportunity to a N_N to read and write multiple bits (a packet) and release drug when required. In this case, the NCU has responsibility for controlling the level of particles and drug in the boxes, if their level is below a certain threshold a request of particles or drug will be sent in the nano-network. This mechanism gives the ability for N_N to always have the capability to communicate and deliver drug when required. Moreover, this enhances the reuse of particles in the network for enabling communications. During the initialisation of the

nano-network, a N_N will have a nano-motor in order to leave the center path of the blood vessel and reach the membrane. This nano-motor will not be used after the N_N becomes static and therefore is not shown in Figure 5. The NCU in a N_N is also equipped with a nano-memory device for storing information [67].

Finally, the architecture of a N_{GW} is shown in Figure 5 in which the capabilities of the N_N are enhanced by including a wireless adapter to transmit information externally. The N_{GW} main functionality is to collect information from the nano-network for reporting its status. For example, it needs to make sure that the N_bs and N_Ns are fully operational. Another important aspect is to synchronise packets in different rings in order to avoid collision, therefore, a packet may be slightly delayed. For this reason, each ring (first or second ring in Figure 1) can be seen as an isolated nano-network and from now on in this work only one ring network will be studied.

It is assumed that when N_Ns and the N_{GW} are injected in the circulatory system, these have their drug reservoirs full, which can be used when required.

IV. PHYSICAL LAYER

To understand the communication process between nano-bots, the medium where the transmission is done needs to be modelled. In this section of the study, the propagation method is established along with the velocity in which the particles are transferred.

A. VELOCITY PROFILE

When a fluid travels through a confined space, the velocity of that fluid experiences a change. Because there is higher friction close to the boundaries, flow speed will decrease in areas close to the boundaries and after time has passed, the flow will develop a velocity profile [68].

$$u(r) = -\frac{R^2}{4\eta}\left(\frac{dP}{dx}\right)\left(1 - \frac{r^2}{R^2}\right) \tag{1}$$

where dP/dx is the pressure loss per distance (Pa/s), R is the radius of the pipe (m), η is the dynamic viscosity ($\mathrm{N \cdot s/m^2}$) and r is the radius of which the velocity is measured (m). As can be seen, the velocity profile in a pipe is parabolic with a maximum velocity occurring in the centreline ($r = 0$), in addition due to the viscous effects, the pressure experiences a decrease in the flow direction, making the pressure drop negative.

In this study the nano-bots are made to travel in the center of the blood vessels, therefore only the maximum flow will be taken into account when modelling the propagation.

B. DIFFUSION

Known as Brownian Motion, diffusion is a process of random particle motion caused by collisions of other fast-moving atoms or particles in aquoeus medium [69], [70]. Even though this process is random propagation in nature, information could be transmitted from one point to another, relying only by using diffusion. The main advantage of this technique is that the energy of the propagation is sourced from thermal energy of its environment and can tap into this energy without any need of an external energy source. Application of this method can be observed in numerous biological processes such as DNA replication, protein production [71] etc. The diffusivity constant in water can be estimated using the Stokes-Einstein relation [72].

$$D = \frac{k_B T}{6\pi\eta r} \tag{2}$$

where k_B is the Boltzmann's constant (J/K), T is the temperature (K), η is the dynamic viscosity ($\mathrm{N \cdot s/m^2}$) and r is the radius of the sphere (m).

To model the propagation where only diffusion occurs, Fick's 2$^{\text{nd}}$ law can be utilized [73]. This phenomenon can be expressed as;

$$\frac{\partial C}{\partial t} = D\left(\frac{\partial^2 C}{\partial x^2} + \frac{\partial^2 C}{\partial y^2} + \frac{\partial^2 C}{\partial z^2}\right) \tag{3}$$

where D is the diffusion coefficient ($\mathrm{cm^2/s}$), C is the concentration at a given point in space ($\mathrm{kg/m^3}$). Therefore the concentration of the molecules is dependent on the spacial coordinates as well at the time $C(t, x, y, z)$.

The partial differential equation (PDE) given in Eq. (3) can have numerous solutions, based on the boundaries of the system. One of the minimalist approaches of solving Eq. (3) is to solve it at the point of release of the chemicals (t_0). If M_0 is the initial number of molecules released from the transmitter at the time t_0 then the initial conditions for the molecular concentration C for 1-D, also known as "thin film solution" in literature, diffusion process can be expressed as;

$$C(|x| > 0, t_0) = 0 \tag{4a}$$

$$C(x = 0, t_0) = M\delta(x) \tag{4b}$$

$$C(|x| \to \infty, t) = 0 \tag{4c}$$

In these equations $\delta(x)$ represents the continuous Dirac delta function for a given spatial dimension (x, y, z) defined as [74]:

$$\int_{-\infty}^{+\infty} \delta(x)dx = 1 \tag{5}$$

By implementing the initial conditions on the PDE, the Eq. (3) can be solved and the solution for the each dimension are;

$$C\,(x, y, z, t) = \frac{M_0}{\sqrt{(4\pi Dt)^3}} \exp\left(-\frac{x^2 + y^2 + z^2}{4Dt}\right) \tag{6}$$

C. ADVECTION

Communication that relies on particles in a aqueous medium follows advective diffusion equation. In literature this is also known as the convection-diffusion equation and the drift-diffusion equation [75] which is expressed as [76];

$$\frac{\partial C}{\partial t} = \underbrace{\overbrace{\nabla \cdot (D\nabla C)}^{\text{Diffusion}} - \overbrace{\nabla \cdot (uC)}^{\text{Advection}}}_{\text{Advection}-\text{Diffusion}} + R \tag{7}$$

where;

- C is the concentration of mass transfer (kg/m^3).
- D is the diffusivity coefficient (i.e. mass diffusivity for particle motion) (m^2/s).
- u is the velocity field that the quantity is moving with (m/s).
- R is the "sinks" or "sources" of the quantity C.

To solve Eq. (7), an approach is to change the frame of reference from stationary coordinates (x, t) to moving coordinates (θ, t). This reference frame can be mathematically expressed as;

$$\theta = (x - u_x t) \tag{8}$$

By substituting from Eq. (8) to Eq. (7) becomes,

$$\frac{\partial C}{\partial t} = D\frac{\partial^2 C}{\partial \theta^2} \tag{9}$$

As can be observed, Eq. (9) is Fick's 2$^{\text{nd}}$ law with only difference being having a moving reference frame θ. By using the same boundary conditions described in Eq. (4) the solution for the equations become;

$$C\,(x, t) = \frac{M_0}{\sqrt{4\pi Dt}} \exp\left(-\frac{\theta^2}{4Dt}\right) \tag{10}$$

Converting back to the stationary frame of reference, the final equation is obtained and the 3D solution can be seen in Eq. (11).

$$C\,(x, y, z, t) = \frac{M_0}{\sqrt{(4\pi Dt)^3}} \exp\left(-\frac{(x - u_x t)^2}{4Dt}\right) \times \exp\left(-\frac{(y - u_y t)^2}{4Dt}\right) \times \exp\left(-\frac{(z - u_z t)^2}{4Dt}\right) \tag{11}$$

The solution above describes an open environment (i.e. no boundaries). However, if this equation needs to be used for a system with boundaries (i.e. blood vessels) the equation must be redefined with initial boundary conditions. By putting $x = r\cos\theta$ and $y = r\sin\theta$ to Eq. (7), the expression can be converted into cylindrical coordinates.

$$\frac{\partial C}{\partial t} = D_L\frac{\partial^2 C}{\partial z^2} - u\frac{\partial C}{\partial z} + \frac{D_R}{r}\left(r\frac{\partial C}{\partial r}\right) \tag{12}$$

where r, θ and z are the cylindrical coordinates. θ is omitted since it is assumed that the system has angular symmetry.

The solution for this kind of equation with initial and boundary conditions can be obtained by implementing Hankel and Laplace Transform [77]. One such solution can be shown below.

$$C(r, z, t) = \frac{\sigma}{\phi\sqrt{D_L \pi t}} \sum_{n=0}^{\infty} \frac{1}{\lambda_n} \times \left(\exp\left(-\frac{(ut - z)^2}{4D_L t} - D_R\lambda_n^2 t\right) - \frac{u}{2D_L}\exp\left(-\frac{uz}{D_L} - D_R\lambda_n^2 t\right)\operatorname{erfc}\left(\frac{z + ut}{\sqrt{4D_L t}}\right)\right) \times \left(\frac{\rho^2}{R^2} + \frac{2\rho J_1(\lambda_n\rho)J_0(\lambda_n r)}{R^2|J_0(\lambda_n R)|^2}\right) \tag{13}$$

where R is the radius of the cylindrical system (m), ρ is the radius of the inner injected zone, σ is the solute mass distribution in the inner inlet zone with instantaneous input (kg/m^2), ϕ is the porosity of the material, D_T is the transverse dispersion coefficient (m^2/h), D_L is the longitudinal dispersion coefficient (m^2/h), λ_n is the Hankel transform parameter determined by the following transcendental equation;

$$\frac{dJ_0(\lambda_n R)}{dr} = 0 \tag{14}$$

As can be seen, defining boundaries on to the propagation greatly increases the complexity of the analytical solution, relying on different methods for solving the PDE, such as separation of variables [78] or change of variables. In the following subsection the physical interactions between nano-bots will be discussed.

D. DOCKING & DEPARTING PROCESS

For information to be transmitted from the travelling nano-bot (N_b) to the stationary (N_N or N_{GW}), the travelling nano-bot has to physically connect to the carbon nano-tubes that are connected to the stationary nano-bots. The docking process and the particle transmission between nano-bots can be seen in Figure 6.

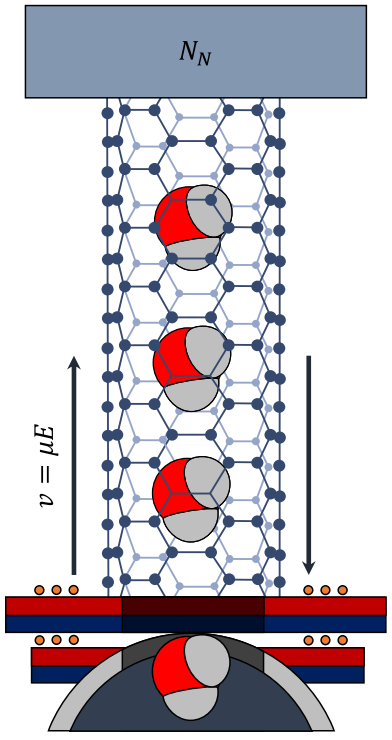

FIGURE 6. A visual representation of the transportation of particles from the travelling nano-bot to the stationary nano-bot.

To realize the docking process, a magnetic locking mechanism is proposed where the configuration can be seen in Figure 7. Recent advancements in material science has allowed the magnets to shrink to nano-scale [53]–[55], with a theoretical size limit of, depending on the material, 3-50 nm [79] at which the magnetization starts to randomly flip its direction due to thermal activation, which marks the superparamagnetic state of the system. For the travelling nano-bot to dock, the poles between the travelling nano-bot and the stationary carbon nano-tube have to be opposite. This creates a magnetic force that allows the docking procedure to occur. The forces acting on the docking and departing procedures can be seen in Figure 7 (A) and (B), This section is split into two section describing the two dimensional forces acting on the nano-bot.

1) AXIAL FORCES (F_z)

In the docking process, the major forces that play a role can be listed as;

- Gravitational forces ($\mathbf{F_G}$)
- Drag force caused by the fluid ($\mathbf{F_D}$)
- Axial magnetic force ($\mathbf{F_z}$)

The gravitational force that is acting on the nano-bot itself can be written as Newton's 2nd law [80].

$$\mathbf{F_G} = m\mathbf{g} \tag{15}$$

where $\mathbf{F_G}$ is the net force applied (N), m is the mass of the nano-bot (kg) and $\mathbf{g}$ is the gravitational constant of the environment (m/s^2).

The second force acting of the nano-bot is the drag force ($\mathbf{F_D}$) (aka. fluid resistance). This is a force acting opposite motion to the body moving and can be represented by the drag equation [68].

$$\mathbf{F_D} = \frac{1}{2}\rho \mathbf{u}^2 C_D A \tag{16}$$

where $\mathbf{F_D}$ is the drag force (N), ρ is the mass density of the fluid (kg/m^3), $\mathbf{u}$ is the flow velocity relative to the object (m/s), A is the reference area (m^2) and C_D is the drag coefficient, which is a dimensionless value related to the objects geometry.

The final force that is acting on the nano-bot, $\mathbf{F_z}$ can be modelled using Amperian current loop models [81]–[83]. The equation for the horizontal magnetic force can be written as;

$$\mathbf{F_z}(I_1, I_2, z) = \frac{\mu_0 I_1 I_2 z}{\sqrt{(R_1+R_2)^2+z^2}} \times \left[\frac{R_1^2+R_2^2+z^2}{(R_1-R_2)^2+z^2}E(k) - K(k)\right] \tag{17}$$

where μ_0 is the magnetic permeability of vacuum (N/A^2), I_1 and I_2 is the current passing through the first and second loop respectively (A), R_1 and R_2 are the radius of the first and second magnets respectively (m), z is the distance between magnets (m), K is the complete elliptic integral of the first kind and E is the complete elliptic integral of the second kind with the following identities.

$$E(k) = \int_0^{\frac{\pi}{2}} \sqrt{1-k^2\sin^2\theta}\, d\theta \tag{18a}$$

$$K(k) = \int_0^{\frac{\pi}{2}} \frac{d\theta}{\sqrt{1-k^2\sin^2\theta}} \tag{18b}$$

$$k = \frac{4R_1R_2}{(R_1+R_2)^2+z^2} \tag{18c}$$

Based on these aforementioned forces acting upon the nano-bot, the resultant force acting on the nano-bot ($\mathbf{F_N}$) can be shown as;

$$\mathbf{F_N} = \mathbf{F_z} - \mathbf{F_D} - \mathbf{F_G} \tag{19a}$$

$$m_N \mathbf{a_N} = \mathbf{F_z} - \mathbf{F_D} - \mathbf{F_G} = \Delta\mathbf{F}_{\text{docking}} \tag{19b}$$

$$\mathbf{a_N} = \frac{\Delta\mathbf{F}_{\text{docking}}}{m_{\text{N}}} \tag{19c}$$

where $\mathbf{a_N}$ is the acceleration occurring on the travelling nano-bot towards to the carbon nano-tube (m/s^2). Therefore the time it takes for the docking process to occur can be calculated as;

$$x_d = \frac{1}{2}\mathbf{a_N} t_d^2 \tag{20a}$$

$$t_{\text{docking}} = \sqrt{\frac{2m_{\text{N}}x_d}{\Delta\mathbf{F}_{\text{docking}}}} \tag{20b}$$

where x_d is the distance between the nano-bot and the carbon nano-tube (m). However, it must be noted, there is a difference between the forces acting on docking and departing processes and that is the gravitational force ($\mathbf{F_G}$) happening on the travelling nano-bot where the force when departing aids in the repelling. This slightly decreases the time in the departing process.

$$\Delta\mathbf{F}_{\text{departing}} = \mathbf{F_z} - \mathbf{F_D} + \mathbf{F_G} \tag{21a}$$

$$t_{\text{departing}} = \sqrt{\frac{2m_{\text{N}}x_d}{\Delta\mathbf{F}_{\text{departing}}}} \tag{21b}$$

Therefore the total time it takes for the departing/docking process to complete (t_{st}) can be simply written as;

$$t_{\text{st}} = \sqrt{\frac{2m_{\text{N}}x_d}{\Delta\mathbf{F}_{\text{docking}}}} + \sqrt{\frac{2m_{\text{N}}x_d}{\Delta\mathbf{F}_{\text{departing}}}} \tag{22}$$

2) LATERAL FORCES (F_x)

As the transmission occurs where there is a constant flow in the environment, the magnetic locking has to be able to withstand the lateral forces acting on the nano-bot. The lateral forces on the travelling nano-bot can be seen in Figure 7 (C).

The first force to mention is the change of momentum on the travelling nano-bot. For the travelling nano-bot to be able to dock, the velocity of the travelling nano-bot needs to drop from the environmental velocity to zero.

$$\mathbf{F_m} = m\frac{\mathrm{d}\mathbf{v}}{\mathrm{d}t} \tag{23}$$

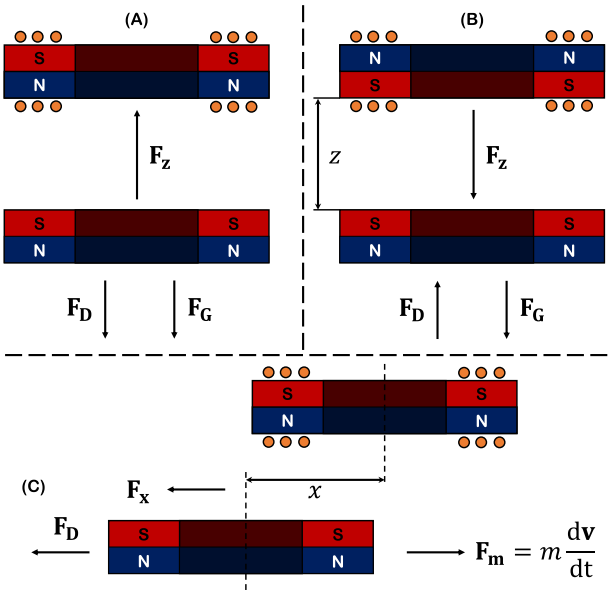

FIGURE 7. A diagram of the possible situation in magnet-to-magnet interactions in docking/departing processes (A) Docking process (B) Departing process (C) Lateral stability.

The second force acting on the travelling nano-bot is the drag forces which is shown in Eq. (16) and the final force is the lateral magnetic force ($\mathbf{F_x}$) shown below [82], [83].

$$F_x(I_1, I_2, x, z) = \frac{I_1 I_2 \mu_0 R_2}{2\pi} \times \int_{-\pi/2}^{\pi/2} [F_s(r_1, x, z) - F_s(r_2, x, z)]\, d\phi \tag{24}$$

where

$$F_s(r, x, z) = \frac{\cos\phi}{\sqrt{(R_1 + r)^2 + z^2}} \times \left(\frac{R_1^2 - r^2 - z^2}{(R_1 - r)^2 + z^2} E[k(r)] - K[k(r)] \right) \tag{25}$$

$$r_1 = \sqrt{(R_2 \cos\phi + x)^2 + (R_2 \sin\phi)^2} \tag{26a}$$

$$r_2 = \sqrt{(R_2 \cos\phi - x)^2 + (R_2 \sin\phi)^2} \tag{26b}$$

$$k(r) = \frac{4R_1 r}{(R_1 + r)^2 + z^2} \tag{26c}$$

Therefore the minimum time which the system takes to slow down can be shown as;

$$\mathbf{F_m} = \mathbf{F_x} - \mathbf{F_D} \tag{27a}$$

$$\int \frac{m}{\mathbf{F_x} - \mathbf{F_D}} d\mathbf{v} = \int dt \tag{27b}$$

$$\frac{m\mathbf{v}}{\mathbf{F_x} - \mathbf{F_D}} = t_{\text{stability}} \tag{27c}$$

where $t_{\text{stability}}$ is the time it takes for the travelling nano-bot to decelerate (s)

E. READ & WRITE PROCESS

Once a connection is physically established between the travelling nano-bot and the static nano-bot, the particles are propagated from the travelling nano-bot via the carbon nanotubes. To increase the propagation an electric field is applied. This process has been used in transporting water via carbon nanotubes [65].

When a charged particle in the liquid medium is acted upon by a uniform electric field it will experience an acceleration until the particle reaches the drift velocity (v_d) defined by the following relation [84].

$$v_d = \mu E \tag{28}$$

where v_d is the drift velocity (m/s), E is the electric field magnitude (V/m) and μ is the mobility (m^2/Vs). The time it takes to travel up and down the nano-tube can be written as;

$$t_n = \frac{2L}{\mu E} \tag{29}$$

In conclusion the total amount of time in the physical layer can simply be written as;

$$t_{\text{PHY}} = \overbrace{\frac{2L}{\mu E}}^{t_n} + \overbrace{\sqrt{\frac{2m_{\text{N}}x_d}{\Delta\mathbf{F}_{\text{docking}}}} + \sqrt{\frac{2m_{\text{N}}x_d}{\Delta\mathbf{F}_{\text{departing}}}}}^{t_{st}} \tag{30}$$

V. MEDIUM ACCESS CONTROL LAYER

Similar to a computer network, the main aim of the medium access control (MAC) layer is to provide a control mechanism for accessing the channel in order to enable N_Ns and the N_{GW} to exchange information. The main properties that the MAC layer needs to ensure is the fairness access to the channel and to avoid collisions of frames. As underlined in Section II, the nano-network can be seen as a ring network with a unidirectional flow, in which a frame is composed of n N_bs. The nano-bots in the network that exchange information are m, $m-1$ N_Ns and a N_{GW}, which from now on will be called nodes (N). Nodes in the network that would like to communicate must be able to uniquely identify each other by using a unique address, called NMAC address. The NMAC addresses present in the nano-network are from 0 to $m-1$. These are pre-configured in the nano-memory in the NCU of N_Ns and the N_{GW} prior their injection in the body.

In the nano-network there is a single channel in which each node can access to for communicating. In this work, a collision-free protocol based on the token ring protocol (IEEE 802.5 [85]) is used for accessing the channel, having only one frame of n bits (the token). The basic idea of a token ring protocol is that only the node having an empty token can transmit information. The token is passed from one to another node by attaching, reading, writing and detaching it in t_{PHY} time. The token circulates around the ring node to node until it reaches the destination node.

The source node knows that the destination node received the information by looking at the token. If the information present in the token is different to the information

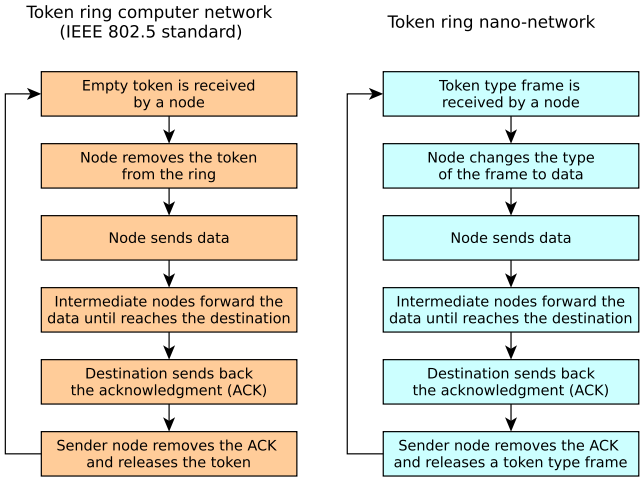

FIGURE 8. **Comparison between the token ring computer network (IEEE 802.5) and the token ring nano-network.**

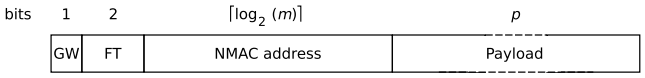

FIGURE 9. **Frame format in the nano-network, where *m* is the number of nodes and *p* is a constant size of the payload.**

sent, the destination has properly received the information (acknowledgement), otherwise the destination is marked as unreachable. In case there is an absence of acknowledgement, the source node empties the token and passes it to the next node, therefore, giving the opportunity for other nodes to transmit information (fairness).

The token in our nano-network differs from the token in the IEEE 802.5 standard by the fact that it can be both a token or a data frame. A comparison between the IEEE 802.5 standard and the proposed nano-network is shown in Figure 8. While in the IEEE 802.5 standard the token becomes a data frame by resizing it, the frame (token or data) in the nano-network has a fixed size ($n\ N_b$) and each N_b arrives at the same time.

The frame format is shown in Figure 9 and it consists of:

- *Gateway bit (GW)*: indicates if the frame is only for the gateway (1) or not (0).
- *Frame type (FT)*: indicates the type of the frame; 0 for the token; 1 for data request (DREQ); and 2 for data response (DREP).
- *NMAC address field*: indicates the unique NMAC address of a node in the nano-network. By default the N_{GW} has a NMAC address with all bits equal to 0.
- *Payload*: this is the payload of a data frame (DREQ or DREP).

The application in a N_N in the nano-network will generate a data frame in two situations: (i) requesting drug or (ii) sending its status and/or sensors data to N_{GW}. To request drug, the application in the N_N will send a DREQ frame. In this frame, the NMAC address field contains the claimant NMAC address (source) and the gateway bit is set to 0, which indicates that the drug is requested from all other nodes (N_{GW}

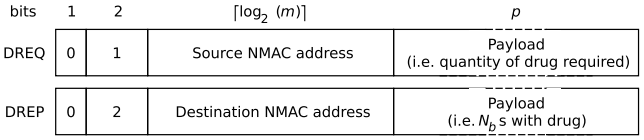

FIGURE 10. **Format of DREQ and DREP frames for drug delivery in the nano-network, where *m* is the number of nodes and *p* is a constant size of the payload.**

included). The format of DREQ frame for requesting drug is shown in Figure 10, in which the payload can contain information that can be useful for improving the communication, for example to describe the quantity of drug required depending on the level of the drug in the reservoir. The quantity of drug (Q_d) that can be delivered is given as;

$$Q_d = 3 + \lceil log_2\,(m) \rceil + p \tag{31}$$

where m is the number of nodes and p is the size of the payload. When a node receives it, its application will check the information in the payload and will release the drug in the N_bs by setting which of them contains the drug. If it does not have the required quantity, it will change the information in the payload, for example by describing the quantity of drug that it is still required and forward it. When a node receives it and it is able to fulfil the request (the quantity in the frame is the same as the requested quantity), it will change the frame type to DREP with the claimant NMAC address (destination) in the NMAC address field as shown in Figure 10. At this point, other intermediate nodes will simply forward the frame until it reaches the destination.

When a N_N needs to send its status and/or sensors data, its application will send a DREQ frame. The payload can contain information that describes the status of the node and/or sensor data, the NMAC address field contains the claimant NMAC address (source) and the gateway bit is set to 1, which indicates that the frame is for the gateway only. Therefore, intermediate nodes will forward the frame until it reaches the gateway. The application in the gateway will extract the information related to the source node and will generate a DREP frame with the NMAC address field containing the NMAC address of the node which generated the frame (acknowledgement).

The time (t_l) required for a frame to travel from one node to the next node (link) is constant and can be expressed as;

$$t_l = \frac{d_l}{v_s} \tag{32}$$

where d_l is a fixed small distance (cm) between two nodes and v_s is the average blood velocity in the aorta, which is equal to $40 \cdot 10^7$ nm/s [86]–[88]. The latency of a transmission (l_l) in a link between two nodes can be calculate as [89];

$$l_l = t_l + t_{\text{PHY}} \tag{33}$$

where t_l is the propagation delay and t_{PHY} is the latency caused by a node for handling the token. As t_l is very small, the limiting factor in l_l is t_{PHY}.

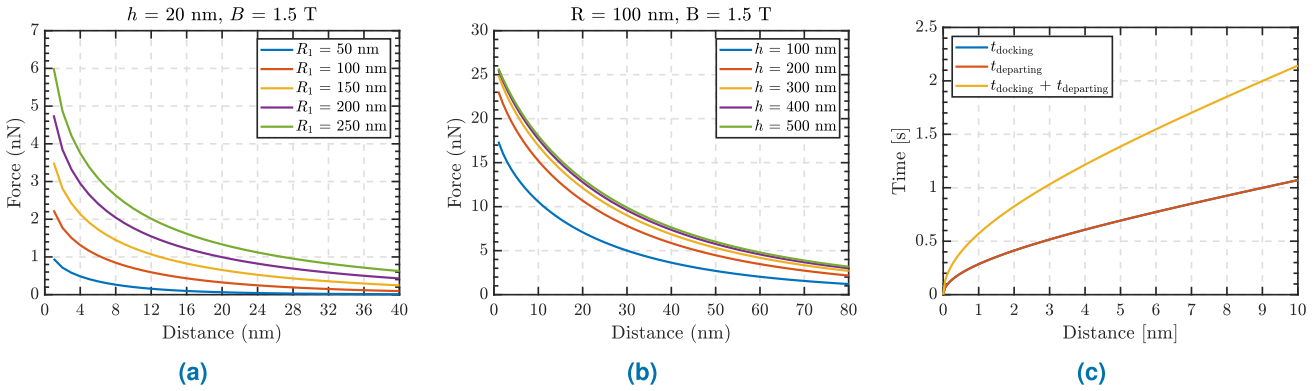

FIGURE 11. Simulation results of magnetic docking process: (a) Results of horizontal magnetic force (F_z) occurring between the two magnets with different radius by varying horizontal distance (x_d) (b) Results of horizontal magnetic force (F_z) occurring between the two magnets with different magnet heights by varying horizontal distance (x_d) (c) Results of the time it takes for the physical interaction between the magnets with respect to the transmission distance.

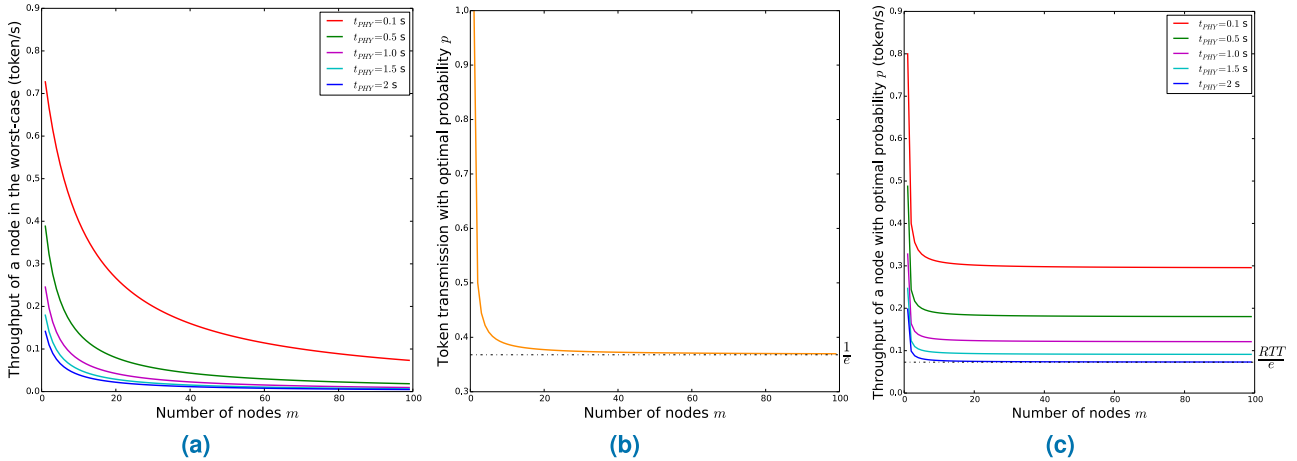

FIGURE 12. (a) Throughput of the nano-network in the worst-case scenario (b) Probability of a successful transmission for a node in the nano-network with optimal p. (c) Throughput of the nano-network with optimal p.

By considering the first ring (Figure 1) with a length (L_r) of around $40 \cdot 10^7$ nm [90], the round-trip time for a token to circulate in the ring and, be handled by the source and the destination nodes, can be calculated as;

$$RTT = \frac{L_r}{v_F} + 2l_l \tag{34}$$

Therefore, the maximum time ($t_{\max}$) required for the token to circulate if all m nodes have information to be transmitted (worst-case) can be calculated as [91];

$$t_{\max} = (m \cdot l_l) + RTT \tag{35}$$

In the worst-case, the effective throughput (token/s) of a node with a free token in the nano-network is given by;

$$T_{\text{worst}} = \frac{1}{t_{\max}} \tag{36}$$

However, not all nodes will always have information to be transmitted. For this reason, in the nano-network the probability for a node to use the token is p. By giving the probability of each of the $m-1$ nodes waiting equal to $1-p$, the value to access the channel is as [92];

$$mp\,(1-p)^{m-1} \tag{37}$$

From which it is possible to derive that the probability of a successful transmission with optimal p is as:

$$\Pr\left[\text{optimal } p\right] = \left[\frac{m-1}{m}\right]^{m-1} \tag{38}$$

From this equation, it is possible to calculate the throughput (token/s) in the nano-network given the optimal probability p as:

$$T_{\text{optimal}} = \frac{\Pr\left[\text{optimal } p\right]}{RTT} \tag{39}$$

VI. RESULTS

In the first part of the section the physical aspect of the communication is analysed and the parameters of the simulation can be seen in Table 1.

TABLE 1. Simulation parameters of magnetic locking process.

Parameter	Symbol	Value	Unit
Permeability of free space [93]	μ_0	$4\pi \times 10^{-7}$	h/m
Magnetic flux density	B	1.5	T
Magnet radius	R	100	nm
Magnet height	h	500	nm
Drag coefficient [94]	C_D	0.42	–
Velocity of blood [90]	v_s	20	cm/s
Density of blood [95]	ρ	1060	kg/m^3
Acceleration of gravity [93]	$\mathbf{g}$	9.81	m/s^2

As mentioned, the magnetic attraction plays an important role in realizing the system and therefore simulation work is carried on the magnetic force between the nano-bots and the horizontal distance (x_d) where the effect of different radii can be observed in Figure 11a and different heights in Figure 11b. As can be seen, the radius and the height play a prominent role in increasing the overall force exerted on to the travelling magnet. A final simulation is done on the physical time it takes the docking/departing to finish and can be seen in Figure 11c. It must be noted that because the gravitational force acting on the nano-bot is minute compared to the magnetic force that its effect on the system is negligible whether the force aids or hinders the magnetic force.

In the second part of the section the behaviours of the nano-network are investigated by varying the number of nodes m present in the network for different values of t_{PHY}. Figure 12a shows the throughput of the nano-network when each node has data to transmit at the same time. It is possible to see that in this situation the increase of m results in a decrease in throughput, reaching 0 when m rises to ∞.

As underlined in Section V, not all nodes will have data to be transmitted and, by using Eq. (38), the probability of a successful transmission with optimal p by varying m is shown in Figure 12b. In here it can be seen that by increasing the number of nodes, the probability of a successful transmission tends to the asymptotic value of $1/e$.

From this result, the throughput of the nano-network with optimal p by varying m and for different values of t_{PHY} is shown in Figure 12c. Therefore, independently by the number of nodes in the nano-network, the throughput will not be worst than RTT/e (token/s).

VII. CONCLUSIONS

This paper presents a concept in which nano-scale communication can be established in in-vivo circulatory systems. To create the information transmission necessary for the network, travelling nano-bots are described which utilize the flow of the blood circulation for their propagation. By using encapsulated drug/information carriers (i.e. nano-bots) the problem of diffusion and unwanted chemical transmission is avoided. Stationary nodes are used to receive environment information, gather data and send this to other stationary nano-bots (packets) using travelling nano-bot. This whole network is defined as a ring network used in traditional computer networks. Based on this topology, a communication protocol is established with the package size and the physical limitations in mind, such as the magnetic docking/departing processes and information transmission between nano-bots. A third nano-bot, nano-bot gateway, is discussed that is used to create a communication link with the outside environment using electromagnetic waves. This is done to increase the security of the communication and to decrease the amount of radiation the body is exposed to. Lastly, simulation work was done on the analysis of the network's performances and was shown to be able to transmit information. Future-work will focus on studying other MAC protocols and above layers and their network analysis in addition to focusing on different environments and their effect on the proposed physical system. We also plan to evaluate the number of maximum N_bs that the system can support which defines the dimension of the token.

REFERENCES

[1] O. C. Farokhzad and R. Langer, "Impact of nanotechnology on drug delivery," *ACS Nano*, vol. 3, no. 1, pp. 16–20, 2009.

[2] G. Orive, R. M. Hernández, A. R. Gascón, A. Domínguez-Gil, and J. L. Pedraz, "Drug delivery in biotechnology: Present and future," *Current Opinion Biotechnol.*, vol. 14, no. 6, pp. 659–664, 2003.

[3] M. C. Tanzi *et al.*, "Trends in biomedical engineering: Focus on smart biomaterials and drug delivery," *J. Appl. Biomaterials Biomech.*, vol. 9, no. 2, pp. 87–97, 2011.

[4] C. S. Joseph, A. N. Yaroslavsky, V. A. Neel, T. M. Goyette, and R. H. Giles, "Continuous wave terahertz transmission imaging of nonmelanoma skin cancers," *Lasers Surg. Med.*, vol. 43, no. 6, pp. 457–462, 2011.

[5] E. Jung *et al.*, "Thz time-domain spectroscopic imaging of human articular cartilage," *J. Infr., Millim., Terahertz Waves*, vol. 33, no. 6, pp. 593–598, 2012.

[6] E. Berry *et al.*, "Optical properties of tissue measured using terahertz-pulsed imaging," *Proc. SPIE*, vol. 5030, pp. 459–471, Jun. 2003.

[7] A. Fitzgerald *et al.*, "Catalogue of human tissue optical properties at terahertz frequencies," *J. Biol. Phys.*, vol. 29, nos. 2–3, pp. 123–128, 2003.

[8] J. M. Jornet and I. F. Akyildiz, "Channel modeling and capacity analysis for electromagnetic wireless nanonetworks in the terahertz band," *IEEE Trans. Wireless Commun.*, vol. 10, no. 10, pp. 3211–3221, Oct. 2011.

[9] G. J. Wilmink and J. E. Grundt, "Invited review article: Current state of research on biological effects of terahertz radiation," *J. Infr., Millim., Terahertz Waves*, vol. 32, no. 10, pp. 1074–1122, Oct. 2011.

[10] *IEEE Standard for Safety Levels with Respect to Human Exposure to Radio Frequency Electromagnetic Fields, 3 kHz to 300 GHz*, IEEE Standard C95.1-2005, 2015.

[11] V. Franchini *et al.*, "Study of the effects of 0.15 terahertz radiation on genome integrity of adult fibroblasts," *Environ. Mol. Mutagenesis*, vol. 59, no. 6, pp. 476–487, 2018.

[12] S. Romanenko, R. Begley, A. R. Harvey, L. Hool, and V. P. Wallace, "The interaction between electromagnetic fields at megahertz, gigahertz and terahertz frequencies with cells, tissues and organisms: Risks and potential," *J. Roy. Soc. Interface*, vol. 14, no. 137, p. 20170585, 2017.

[13] A. De Amicis *et al.*, "Biological effects of *in vitro* THz radiation exposure in human foetal fibroblasts," *Mutation Res./Genetic Toxicol. Environ. Mutagenesis*, vol. 793, pp. 150–160, Nov. 2015.

[14] L. V. Titova *et al.*, "Intense THz pulses cause H2AX phosphorylation and activate DNA damage response in human skin tissue," *Biomed. Opt. Express*, vol. 4, no. 4, pp. 559–568, 2013.

[15] Y. Yamaguchi *et al.*, "Human skin responses to UV radiation: Pigment in the upper epidermis protects against dna damage in the lower epidermis and facilitates apoptosis," *FASEB J.*, vol. 20, no. 9, pp. 1486–1488, 2006.

[16] N. G. Jablonski and G. Chaplin, "Human skin pigmentation as an adaptation to UV radiation," *Proc. Nat. Acad. Sci. USA*, vol. 107, pp. 8962–8968, May 2010.

[17] S. Hiyama *et al.*, "Molecular communication," *J.-Inst. Electron. Inf. Commun. Eng.*, vol. 89, no. 2, p. 162, 2006.
[18] M. Pierobon and I. F. Akyildiz, "A physical end-to-end model for molecular communication in nanonetworks," *IEEE J. Sel. Areas Commun.*, vol. 28, no. 4, pp. 602–611, May 2010.
[19] M. C. S. Kuran, H. B. Yilmaz, T. Tugcu, and B. Özerman, "Energy model for communication via diffusion in nanonetworks," *Nano Commun. Netw.*, vol. 1, no. 2, pp. 86–95, 2010.
[20] M. Pierobon and I. F. Akyildiz, "Diffusion-based noise analysis for molecular communication in nanonetworks," *IEEE Trans. Signal Process.*, vol. 59, no. 6, pp. 2532–2547, Jun. 2011.
[21] D. T. McGuiness, S. Giannoukos, A. Marshall, and S. Taylor, "Parameter analysis in macro-scale molecular communications using advection-diffusion," *IEEE Access*, vol. 6, pp. 46706–46717, 2018.
[22] D. T. McGuiness, S. Giannoukos, A. Marshall, and S. Taylor, "Experimental results on the open-air transmission of macro-molecular communication using membrane inlet mass spectrometry," *IEEE Commun. Lett.*, vol. 22, no. 12 pp. 2567–2570, Dec. 2018.
[23] D. McGuiness, A. Marshall, S. Taylor, and S. Giannoukos, "Asymmetrical inter-symbol interference in macro-scale molecular communications," in *Proc. 5th ACM Int. Conf. Nanosc. Comput. Commun.*, 2018, Art. no. 13.
[24] N. Farsad, H. B. Yilmaz, A. Eckford, C.-B. Chae, and W. Guo, "A comprehensive survey of recent advancements in molecular communication," *IEEE Commun. Surveys Tuts.*, vol. 18, no. 3, pp. 1887–1919, 3rd Quart., 2016.
[25] S. Giannoukos, D. T. McGuiness, A. Marshall, J. Smith, and S. Taylor, "A chemical alphabet for macromolecular communications," *Anal. Chem.*, vol. 90, no. 12, pp. 7739–7746, 2018.
[26] P. I. Aaronson, J. P. T. Ward, and M. J. Connolly, *The Cardiovascular System at a Glance*. Hoboken, NJ, USA: Wiley, 2012.
[27] L. Felicetti, M. Femminella, G. Reali, and P. Liò, "Applications of molecular communications to medicine: A survey," *Nano Commun. Netw.*, vol. 7, pp. 27–45, Mar. 2016.
[28] Y. Chahibi, "Molecular communication for drug delivery systems: A survey," *Nano Commun. Netw.*, vol. 11, pp. 90–102, Mar. 2017.
[29] X. Dong, "Current strategies for brain drug delivery," *Theranostics*, vol. 8, no. 6, pp. 1481–1493, 2018.
[30] Y. Chen and L. Liu, "Modern methods for delivery of drugs across the blood–brain barrier," *Adv. Drug Del. Rev.*, vol. 64, no. 7, pp. 640–665, May 2012.
[31] L. A. Khawli and S. Prabhu, "Drug delivery across the blood–brain barrier," *Mol. Pharmaceutics*, vol. 10, no. 5, pp. 1471–1472, 2013, doi: 10.1021/mp400170b.
[32] E. Blanco, H. Shen, and M. Ferrari, "Principles of nanoparticle design for overcoming biological barriers to drug delivery," *Nature Biotechnol.*, vol. 33, no. 9, pp. 941–951, 2015.
[33] Y. Zhou, Z. Peng, E. S. Seven, and R. M. Leblanc, "Crossing the blood-brain barrier with nanoparticles," *J. Controlled Release*, vol. 270, pp. 290–303, Jan. 2017.
[34] C. Saraiva, C. Praça, R. Ferreira, T. Santos, L. Ferreira, and L. Bernardino, "Nanoparticle-mediated brain drug delivery: Overcoming blood-brain barrier to treat neurodegenerative diseases," *J. Controlled Release*, vol. 235, pp. 34–47, Aug. 2016.
[35] S. Jin and K. Ye, "Nanoparticle-mediated drug delivery and gene therapy," *Biotechnol. Prog.*, vol. 23, no. 1, pp. 32–41, 2007.
[36] J. P. Renaud *et al.*, "Biophysics in drug discovery: Impact, challenges and opportunities," *Nature Rev. Drug Discovery*, vol. 15, no. 10, pp. 679–698, 2016.
[37] L. N. Ramana, A. R. Anand, S. Sethuraman, and U. M. Krishnan, "Targeting strategies for delivery of anti-HIV drugs," *J. Controlled Release*, vol. 192, pp. 271–283, Oct. 2014.
[38] R. Mittal *et al.*, "Recent advancements in nanoparticle based drug delivery for gastrointestinal disorders," *Expert Opinion Drug Del.*, vol. 15, no. 3, pp. 301–318, 2018.
[39] H. Laroui, S. V. Sitaraman, and D. Merlin, "Gastrointestinal delivery of anti-inflammatory nanoparticles," in *Methods in Enzymology*, vol. 509. Amsterdam, The Netherlands: Elsevier, 2012, pp. 101–125.
[40] I. F. Akyildiz, F. Brunetti, and C. Blázquez, "Nanonetworks: A new communication paradigm," *Comput. Netw.*, vol. 52, no. 12, pp. 2260–2279, 2008.
[41] A. Gupta, M. Medley, and J. M. Jornet, "Joint synchronization and symbol detection design for pulse-based communications in the THz band," in *Proc. IEEE Global Commun. Conf. (GLOBECOM)*, Dec. 2015, pp. 1–7.
[42] I. F. Akyildiz, J. M. Jornet, and C. Han, "Terahertz band: Next frontier for wireless communications," *Phys. Commun.*, vol. 12, pp. 16–32, Sep. 2014.
[43] J. Lin, X. Lin, and L. Tang, "Making-a-stop: A new bufferless routing algorithm for on-chip network," *J. Parallel Distrib. Comput.*, vol. 72, no. 4, pp. 515–524, Apr. 2012.
[44] Z. Zhang, Z. Guo, and Y. Yang, "Bufferless routing in optical Gaussian macrochip interconnect," *IEEE Trans. Comput.*, vol. 63, no. 11, pp. 2685–2700, Nov. 2014.
[45] J. M. Jornet, J. C. Pujol, and J. S. Pareta, "PHLAME: A physical layer aware MAC protocol for electromagnetic nanonetworks in the terahertz band," *Nano Commun. Netw.*, vol. 3, no. 1, pp. 74–81, 2012.
[46] P. Wang, J. M. Jornet, M. A. A. Malik, N. Akkari, and I. F. Akyildiz, "Energy and spectrum-aware MAC protocol for perpetual wireless nanosensor networks in the Terahertz band," *Ad Hoc Netw.*, vol. 11, no. 8, pp. 2541–2555, 2013.
[47] S. Mohrehkesh and M. C. Weigle, "RIH-MAC: Receiver-initiated harvesting-aware MAC for nanonetworks," in *Proc. ACM 1st Annu. Int. Conf. Nanosc. Comput. Commun.*, 2014, Art. no. 6.
[48] Q. Xia, Z. Hossain, M. Medley, and J. M. Jornet, "A link-layer synchronization and medium access control protocol for terahertz-band communication networks," in *Proc. IEEE Global Commun. Conf. (GLOBECOM)*, Dec. 2015, pp. 1–7.
[49] J. Tan, A. Thomas, and Y. Liu, "Influence of red blood cells on nanoparticle targeted delivery in microcirculation," *Soft Matter*, vol. 8, no. 6, pp. 1934–1946, 2012.
[50] L. Felicetti, M. Femminella, and G. Reali, "Simulation of molecular signaling in blood vessels: Software design and application to atherogenesis," *Nano Commun. Netw.*, vol. 4, no. 3, pp. 98–119, Sep. 2013.
[51] X. Huang, P. Craig, H. Lin, and Z. Yan, "SecIoT: A security framework for the Internet of Things," *Secur. Commun. Netw.*, vol. 9, no. 16, pp. 3083–3094, 2016.
[52] F. Dressler and F. Kargl, "Towards security in nano-communication: Challenges and opportunities," *Nano Commun. Netw.*, vol. 3, no. 3, pp. 151–160, 2012.
[53] F. Donati *et al.*, "Magnetic remanence in single atoms," *Science*, vol. 352, no. 6283, pp. 318–321, 2016.
[54] N. Ishikawa, M. Sugita, and W. Wernsdorfer, "Nuclear spin driven quantum tunneling of magnetization in a new lanthanide single-molecule magnet: Bis(phthalocyaninato)holmium anion," *J. Amer. Chem. Soc.*, vol. 127, no. 11, pp. 3650–3651, 2005.
[55] P. Gambardella *et al.*, "Giant magnetic anisotropy of single cobalt atoms and nanoparticles," *Science*, vol. 300, no. 5622, pp. 1130–1133, 2003.
[56] G. Hwang *et al.*, "Electro-osmotic propulsion of helical nanobelt swimmers," *Int. J. Robot. Res.*, vol. 30, no. 7, pp. 806–819, 2011.
[57] H. Wang and M. Pumera, "Fabrication of micro/nanoscale motors," *Chem. Rev.*, vol. 115, no. 16, pp. 8704–8735, Aug. 2015.
[58] Z. L. Wang and J. Song, "Piezoelectric nanogenerators based on zinc oxide nanowire arrays," *Science*, vol. 312, pp. 242–246, Apr. 2006.
[59] Z. L. Wang, G. Zhu, Y. Yang, S. Wang, and C. Pan, "Progress in nanogenerators for portable electronics," *Mater. Today*, vol. 15, no. 12, pp. 532–543, 2012.
[60] J. Briscoe and S. Dunn, "Piezoelectric nanogenerators—A review of nanostructured piezoelectric energy harvesters," *Nano Energy*, vol. 14, pp. 15–29, May 2015.
[61] Y. Hu, J. Xiang, G. Liang, H. Yan, and C. M. Lieber, "Sub-100 nanometer channel length Ge/Si nanowire transistors with potential for 2 THz switching speed," *Nano Lett.*, vol. 8, no. 3, pp. 925–930, 2008.
[62] H. Yan *et al.*, "Programmable nanowire circuits for nanoprocessors," *Nature*, vol. 470, no. 7333, pp. 240–244, 2011.
[63] X. Wang, J. Zhou, J. Song, J. Liu, N. Xu, and Z. L. Wang, "Piezoelectric field effect transistor and nanoforce sensor based on a single ZnO nanowire," *Nano Lett.*, vol. 6, no. 12, pp. 2768–2772, 2006.
[64] Y. Gogotsi and R. M. Penner, "Energy storage in nanomaterials—Capacitive, pseudocapacitive, or battery-like?" *ACS Nano*, vol. 12, no. 3, pp. 2081–2083, 2018.
[65] K. Ritos, M. K. Borg, N. J. Mottram, and J. M. Reese, "Electric fields can control the transport of water in carbon nanotubes," *Philos. Trans. Roy. Soc. London A, Math. Phys. Sci.*, vol. 374, no. 2060, p. 20150025, 2016.
[66] X. Wang *et al.*, "Fabrication of ultralong and electrically uniform single-walled carbon nanotubes on clean substrates," *Nano Lett.*, vol. 9, no. 9, pp. 3137–3141, Aug. 2009.
[67] A. Chung, J. Deen, J.-S. Lee, and M. Meyyappan, "Nanoscale memory devices," *Nanotechnology*, vol. 21, no. 41, p. 412001, 2010.

[68] Y. A. Cengel, *Fluid Mechanics*. New York, NY, USA: McGraw-Hill, 2010.
[69] R. P. Feynman, R. B. Leighton, and M. Sands, *The Feynman Lectures on Physics*, vol. 1. New York, NY, USA: Basic Books, 2013.
[70] S. Kadloor, R. S. Adve, and A. W. Eckford, "Molecular communication using Brownian motion with drift," *IEEE Trans. Nanobiosci.*, vol. 11, no. 2, pp. 89–99, Jun. 2012.
[71] H. C. Berg, *Random Walks in Biology*. Princeton, NJ, USA: Princeton Univ. Press, 1993.
[72] J. T. Edward, "Molecular volumes and the Stokes–Einstein equation," *J. Chem. Edu.*, vol. 47, no. 4, p. 261, 1970.
[73] J. Crank, *The Mathematics Of Diffusion*. Oxford, U.K.: Oxford Univ. Press, 1979.
[74] I. M. Gel'Fand and G. Shilov, *Spaces of Fundamental and Generalized Functions*, vol. 2. New York, NY, USA: Academic, 1968.
[75] S. Chandrasekhar, "Stochastic problems in physics and astronomy," *Rev. Mod. Phys.*, vol. 15, no. 1, p. 1, 1943.
[76] T. Stocker, *Introduction to Climate Modelling*. Berlin, Germany: Springer, 2011.
[77] J.-S. Chen, Y.-H. Liu, C.-P. Liang, C.-W. Liu, and C.-W. Lin, "Exact analytical solutions for two-dimensional advection–dispersion equation in cylindrical coordinates subject to third-type inlet boundary condition," *Adv. Water Resour.*, vol. 34, no. 3, pp. 365–374, 2011.
[78] N. A. Gershenfeld and N. Gershenfeld, *The Nature of Mathematical Modeling*. Cambridge, U.K.: Cambridge Univ. Press, 1999.
[79] A. Sukhov, L. Chotorlishvili, P. P. Horley, C.-L. Jia, S. K. Mishra, and J. Berakdar, "On the superparamagnetic size limit of nanoparticles on a ferroelectric substrate," *J. Phys. D, Appl. Phys.*, vol. 47, no. 15, p. 155302, 2014.
[80] R. P. Feynman, R. B. Leighton, and M. Sands, *The Feynman Lectures on Physics: Mainly Mechanics, Radiation and Heat*, vol. 1. New York, NY, USA: Basic Books, 2011.
[81] J. R. Hull and A. Cansiz, "Vertical and lateral forces between a permanent magnet and a high-temperature superconductor," *J. Appl. Phys.*, vol. 86, no. 11, pp. 6396–6404, Dec. 1999.
[82] A. Cansiz and D. T. McGuiness, "Optimization of the force and stiffness in a superconducting magnetic bearing based on particular permanent-magnet superconductor configuration," *IEEE Trans. Appl. Supercond.*, vol. 28, no. 2, Mar. 2018, Art. no. 5201208.
[83] A. Cansiz, I. Yildizer, and D. T. McGuiness, "A case study for a superconducting magnetic bearing optimization," in *Proc. IEEE 10th Int. Conf. Elect. Electron. Eng. (ELECO)*, Nov./Dec. 2017, pp. 1466–1470.
[84] C. Canali, C. Jacoboni, F. Nava, G. Ottaviani, and A. Alberigi-Quaranta, "Electron drift velocity in silicon," *Phys. Rev. B, Condens. Matter*, vol. 12, no. 6, p. 2265, 1975.
[85] *Token Ring Access Method and Physical Layer Specifications Fibre Optic Media*, IEEE Standard IEEE 802.5j-1997, ASW Group, 1985.
[86] G. J. Tortora and B. Derrickson, "The cardiovascular system: Blood vessels and hemodynamics," in *Principles of Anatomy and Physiology*, 13th ed. Hoboken, NJ, USA: Wiley, 2011, ch. 21, pp. 802–874.
[87] S. E. Gisvold and A. O. Brubakk, "Measurement of instantaneous blood-flow velocity in the human aorta using pulsed Doppler ultrasound," *Cardiovascular Res.*, vol. 16, no. 1, pp. 26–33, 1982.
[88] H. G. Bogren and M. H. Buonocore, "4D magnetic resonance velocity mapping of blood flow patterns in the aorta in young vs. elderly normal subjects," *J. Magn. Reson. Imag., Off. J. Int. Soc. Magn. Reson. Med.*, vol. 10, no. 5, pp. 861–869, 1999.
[89] W. Bux, "Local-area subnetworks: A performance comparison," *IEEE Trans. Commun.*, vol. COM-29, no. 10, pp. 1465–1473, Oct. 1981.
[90] S. Singhal, R. Henderson, K. Horsfield, K. Harding, and G. Cumming, "Morphometry of the human pulmonary arterial tree," *Circulat. Res.*, vol. 33, no. 2, pp. 190–197, 1973.
[91] A. S. Sethi and T. Saydam, "Performance analysis of token ring local area networks," *Comput. Netw. ISDN Syst.*, vol. 9, no. 3, pp. 191–200, 1985.
[92] A. S. Tanenbaum and D. J. Wetherall, *Computer Networks*, 5th ed. Upper Saddle River, NJ, USA: Prentice-Hall, 2011.
[93] E. R. Cohen, "Fundamental physical constants," in *Gravitational Measurements, Fundamental Metrology and Constants*. Dordrecht, The Netherlands: Springer, 1988, pp. 59–89.
[94] A. Hölzer and M. Sommerfeld, "New simple correlation formula for the drag coefficient of non-spherical particles," *Powder Technol.*, vol. 184, no. 3, pp. 361–365, 2008.
[95] T. Kenner, "The measurement of blood density and its meaning," *Basic Res. Cardiol.*, vol. 84, no. 2, pp. 111–124, 1989.

DANIEL TUNÇ MCGUINESS received the degree in electrical engineering from Istanbul Technical University, in 2016, where he took a final-year specialization in solid-rotor induction motors. He is currently pursuing the Ph.D. degree with the Department of Electrical Engineering and Electronics, University of Liverpool, with a focus on research in macro-scale molecular communications. He was an intern with the Jožef Stefan Institute, Slovenia, in 2014, where he was involved in the aspects of fuel cells and energy-storage systems. Apart from molecular communications, his interests lie in superconductors, energy-storage systems, and electrical machines.

VALERIO SELIS (S'13–M'18) received the B.Sc. and M.Sc. degrees in computer science from the Università degli Studi di Cagliari, Cagliari, Sardinia, Italy, in 2008 and 2011, respectively, and the Ph.D. degree in electrical engineering and electronics from the University of Liverpool, Liverpool, U.K., in 2018. He was a Research Assistant on the Cross-Layer Techniques for Intrusion Tolerant Network Design Project with Queen's University Belfast, Belfast, U.K. Since 2016, he has been the Development Director at Traffic Observation & Management (TOM) Ltd. TOM is a company specialized in intrusion detection and prevention systems for wireless networks. He is currently a Research Associate with the Advanced Networks Research Group, University of Liverpool. His research interests include computer networks, wireless communications, the Internet of Things, network security, trust management, and machine-to-machine communications.

ALAN MARSHALL (M'88–SM'00) holds the Chair in communications networks with the University of Liverpool, where he is also the Director of the Advanced Networks Group and the Head of the Department. He has spent over 24 years working in the telecommunications and defence industries. He has published over 200 scientific papers and holds a number of joint patents in the areas of communications and network security. He has formed a successful spin-out company Traffic Observation and Management Ltd. His research interests include network architectures and protocols, mobile and wireless networks, network security, QoS/QoE architectures, and multisensory communications, including haptics and olfaction. He is a Fellow of the Institution of Engineering and Technology and a Senior Fellow of the Higher Education Academy. He is currently a Section Editor of the *Computer Journal* of the British Computer Society.